Contribution No. 89-131

This report was prepared for the Committee for the Measurement of Flow Under Ice, Water Survey of Canada, Water Resources Branch, Ottawa, Ontario.

A NEW CALIBRATION EQUATION FOR VERTICAL AXIS CURRENT METERS

by
Peter Engel

Research and Applications Branch
National Water Research Institute
Canada Centre for Inland Waters
867 Lakeshore Road, P.O. Box 5050
Burlington, Ontario, Canada L7R 4A6

September 1989

MANAGEMENT PERSPECTIVE

Current meter calibrations are done on a regular basis to ensure that the measurement of streamflow velocity can be made as accurately as possible. A new current meter equation has been developed which will make it possible to obtain greater accuracy of low velocity measurements than has previously been possible. The increased accuracy at the lower velocity is particularly desirable in view of increasing concerns regarding toxic chemical concentrations and loadings in Canadian Rivers. This study is part of an overall quality assurance program presently being conducted by the Water Survey of Canada, through its Committee for the Measurement of Flow Under Ice, with active participation of the National Water Research Institute, in an effort to improve standards and update measuring equipment.

Dr. J. Lawrence
Director
Research and Applications Branch

PERSPECTIVE-GESTION

On procède régulièrement à des étalonnages des courantomètres, de manière à garantir la plus grande précision possible dans la mesure des vitesses d'écoulement. Il a été établi une nouvelle équation de courantomètre qui donne une précision des mesures à basse vitesse bien supérieure à ce qui était possible jusqu'ici. À basse vitesse, il est particulièrement souhaitable d'avoir une bonne précision, car on s'inquiète de plus en plus des concentrations et charges en substances chimiques toxiques dans les cours d'eau du Canada.

Cette étude se situe dans un programme global d'assurance de la qualité présentement réalisé par la Division des relevés hydrologiques du Canada, par l'intermédiaire de son comité de mesure des débits sous la glace, avec la participation active de l'Institut national de recherche sur les eaux. Ce programme découle d'un effort d'amélioration des normes et de mise à jour des appareils de mesure.

Dr. J. Lawrence
Directeur
Direction de la recherche pure et appliquée

SUMMARY

A new calibration equation for the Price current meter with rod suspension has been developed using physical principles and dimensional analysis. The physical parameters which govern the performance of the meter rotor have been revealed and combined into dimensionless coefficients. Excellent agreement between the equation and new calibration data obtained in the NWRI towing tank has been obtained over the range of velocities from 3 cm/s to 300 cm/s. Agreement with the data at velocities less than 40 cm/s was superior to methods presently being used.

RÉSUMÉ

On a établi, à l'aide de principes physiques et par le biais de l'analyse dimensionnelle, une nouvelle équation d'étalonnage du courantomètre de Price monté sur tige. Les paramètres physiques qui régissent le rendement du rotor du courantomètre ont été combinés en coefficients sans dimension. À des vitesses de 3 cm/s à 300 cm/s, il y a une excellente correspondance entre l'équation et les nouvelles données d'étalonnage obtenues dans le bassin d'essai des carènes de l'INRE. Pour les vitesses inférieures à 40 cm/s, la correspondance avec les données est supérieure à ce qu'elle était dans le cas des méthodes utilisées jusqu'ici.

TABLE OF CONTENTS

1.0 INTRODUCTION

The collection, computation and publication of river discharge data are an important part of a national program conducted by the Water Resources Branch (WRB) through the Water Survey of Canada (WSC). The data are used for environmental assessments, design of river works, water supply structures, pollution control, flood control and projects related to navigation and recreation. Increased awareness of river pollution and the importance of water quality monitoring has made it necessary to improve the accuracy of discharge measurements. To meet this objective, a long term study was developed by the WSC.

The determination of river discharge requires the measurement of the flow velocity. The velocity is measured by placing a meter into the flow and recording the rate of rotation of the rotor, usually in revolutions per second. The relationship between the linear velocity of the flow and the revolutions per second is determined by calibrating the meter in a towing tank. The current meter calibrations are normally expressed by some form of equation from which calibration tables are prepared for use in the field.

The present practice of the United States Geological Survey (USGS) (Smoot and Carter, 1968) and the WSC is to fit linear equations to the calibration data. Such methods do not take into account the non-linear behaviour of the current meter which is most pronounced at the low velocities. This report presents the development of a new calibration equation based on physical and dimensional analysis. The equation is compared with the equations used by the USGS and the WSC using calibration data obtained in the towing tank at the National Water Research Institute (NWRI) at Burlington, Ontario. The work was done for the Hydrometric Methods Section of the WSC in Ottawa by the Research and Applications Branch (RAB) of NWRI in accordance with the research and development plan of the Committee for Measurement of Flows Under Ice.

2.0 ANALYTICAL CONSIDERATIONS

The linear velocity of the flow in a stream is measured by placing a current meter into the flow and recording the rate of rotation of the rotor. The relationship between the linear velocity and the revolutions per second is normally determined by calibrating the meter in a towing tank. The calibration is expressed as an equation which is then used to prepare rating tables for use in the field.

2.1 Current Meter Without Friction

The rotor of the Price meter is an assembly of six conical cups mounted symetrically about the vertical axis of rotation as shown in Figure 1. The forces which govern the rotation of the rotor are the drag forces on the stoss-side and the lee-side of the conical elements. These forces create torques about the centre of rotation as shown in Figure 2. For a given steady flow velocity, the meter turns at a constant rate and therefore the balance of the opposing torques may be written as

$$\tfrac{1}{2}\,\rho C_{D1}A(V-\omega r)^2 r - \tfrac{1}{2}\,\rho C_{D2}A(V+\omega r)^2 r = 0 \qquad (1)$$

in which ρ = the density of the fluid, A = the average "bluff-body" area of the conical elements, V = the average flow velocity, r = the effective radius of the rotor as shown in Figure 2, ω = the angular velocity of the rotor and C_{D1} and C_D2 are the drag coefficients of the conical elements on the stoss-side and lee-side respectively. After some simplification and rearranging of variables, equation (1) may be written as

$$V = \left[\frac{\sqrt{C_{D1}} + \sqrt{C_{D2}}}{\sqrt{C_{D1}} - \sqrt{C_{D2}}}\right] \qquad (2)$$

The angular velocity can be related to the rate of rotation N in revolutions per second by the relationship

$$\omega r = \Pi DN \qquad (3)$$

where $\Pi = 3.14....$, D = effective diameter of the rotor (ie: D = 2r) and the other variables have already been defined. Substituting equation (3) into equation (2) and further simplification results in

$$\frac{ND}{v} = \frac{1}{\Pi}\left[\frac{K-1}{K+1}\right] \qquad (4)$$

in which $K = C_{D1}/C_{D2}$. The value of K must be determined experimentally. Equation (4) reflects the typical response characteristics of the Price current meter in a two dimensional flow field if there is no frictional resistance in the bearings and other contact surfaces. ND/V is dependent only on the value of K which reflects the shape and orientation of the conical elements of the rotor. The sensitivity of the meter is dependent on both D and K. The sensitivity can be increased by reducing D and increasing K because the rate of rotation of the rotor will be increased for a given value of the flow velocity. For a given meter the value of K and D are constant and thus the frictionless calibration equation may be further reduced to give

$$V = m\,N \qquad (5)$$

where m is the meter constant. Equation (5) is linear, with slope m and passes through the origin of a V vs. N plot. Such a behaviour would be ideal for a current meter. It is known, however, that calibration curves are nonlinear, particularly in the region of lower velocities. This effect can best be illustrated with the plot of ND/V vs. V in Figure (3). The average curve fitted to the data shows that the meter response is very nonlinear for velocities less than about 30 cm/s. For velocities greater than 30 cm/s the values of ND/V are approximately constant, indicating that the rotor response in this range tends to be linear. The non - linearity of the rotor response manifests itself in the standard V vs. N format of the calibration equations by the departure from the curve for the frictionless meter as shown schematically in Figure 4. The nonlinearity is not observable in a standard V vs. N plot because of the scale that is normally adopted. However, the magnitude of the nonlinearity increases as the density of the fluid decreases. Engel (1976) calibrated Price type current meters in both water and air, for which data are plotted in Figure 5. Curves fitted to the data show virtually no discernible nonlinearity when the fluid is water, whereas in the case of air the nonlinearity is very pronounced. It is also interesting to note in Figure 5 that both curves merge into a single curve indicating that the meter behaves similarly in all Newtonian fluids in the range where the factors contributing to the nonlinearity become insignificantly small.

The non-linearity in the calibration equation is the result of frictional resistance due to the bearings and electrical contact brushes in the meter head as well as possible effects of the meter yoke on the local flow field. These factors cannot be defined theoretically and one must therefore resort to more empirical methods through dimensional analysis.

2.2 Current Meter with Friction

The variables governing the operation of a current meter that are important in the developement of a calibration equation can be expressed by the following set:

$$V, T, N, D, \rho, \mu, \gamma \qquad (6)$$

where T is the resisting torque as a result of friction in the bearings and other contact surfaces, γ = the specific weight of the water, μ = the dynamic viscosity of the water and all other variables have already been defined. Using the Buckingham Pi theorem, the variables in set (6) can be expressed in dimensionless form in the following set:

$$\frac{\rho V^2}{\gamma D}, \quad \frac{T}{\gamma D^4}, \quad \frac{\sqrt{\rho D}\, N}{\sqrt{\gamma}}, \quad \frac{\gamma D^3 \rho}{\mu^2} \tag{7}$$

It was shown by Engel (1976) and Schubauer and Mason (1937) that the effects of viscosity are not important. In addition the density of water does not change significantly over the range of temperature encountered during most flow measurements (Hunter Rouse, 1950). Therefore the variable $\gamma D^3 \rho/\mu^2$ can be considered to be constant and can be eliminated from further considerations. The remaining three dimensionless variables can then be used to form a dimensionless calibration equation given by

$$\frac{\sqrt{\rho}\, V}{\sqrt{\gamma D}} = f_1 \left[\sqrt{\frac{\rho D}{\gamma}} N, \ \frac{T}{\gamma D^4} \right] \tag{8}$$

in which f_1 denotes a function. Recalling Figure 4, it can be seen that a complete calibration curve is equivalent to the sum of two components; the linear frictionless component and the nonlinear friction component. Using this concept, a possible form of the functional relationship of equation (8) can be written as

$$\frac{\sqrt{\rho}\, V}{\sqrt{\gamma D}} = a \sqrt{\frac{\rho D}{\gamma}} N + b \frac{T}{\gamma D^4} \tag{9}$$

in which a and b are coefficients. The nonlinear component must vary in some way with N. When $N = 0$, the nonlinear component reaches its maximum value. As N increases from zero, contribution of the nonlinear component declines with the rate of change decreasing as N increases. Since γ, D and b are constant, then for a given fluid, the variation must be due to the variable T. A relationship for T which meets the required criteria is given as

$$T = T_0 \; e^{-kN} \tag{10}$$

where T_0 is the resistance in the meter at the point of beginning of rotation of the rotor which occurs at the threshold velocity (ie: when $N = 0$) and k is a coefficient which has the units so as to make the exponent kN dimensionless. Combining equations (9) and (10) and simplifying results in

$$V = aDN + \frac{bT_0 e^{-kN}}{\sqrt{\rho\gamma} \; D^{7/2}} \tag{11}$$

For a given meter γ and D are constant. It is also known that ρ does not vary significantly over the range of water temperatures encountered during flow measurements. Also for a given meter the value of T_0 is constant as long as the meter adjustment at the time of calibration is not disturbed. Therefore, equation (11) can be written in the general form as

$$V = AN + Be^{-kN} \tag{12}$$

where A, B and k are coefficients.

Comparison of equations (4),(5),(11) and (12) shows that the coefficients A, and B are given by

$$A = \left[\frac{k+1}{k-1}\right]\frac{D}{\Pi} \qquad B = \frac{b\,T_0}{\sqrt{\rho\gamma}\,D^{7/2}} \qquad (13)$$

2.2.1 The effect of A

It can be seen from the above relationships that A depends on the shape and orientation of the conical elements of the rotor as was the case for the frictionless equation. Physically, A represents the equivalent pitch of the rotor of a frictionless meter, which is defined as the distance through which the meter must be towed to achieve one complete revolution. The size of the pitch is an indicator of the sensitivity of the meter. In comparing two meters, the meter having the smaller pitch has the greater sensitivity. In other words for an equal change in velocity, the meter with the smaller pitch will have a larger change in the rate of rotation of the rotor.

2.2.2 The effect of B

The coefficient B represents the threshold velocity of the meter. Theoretically, the threshold velocity is the maximum velocity for which the rotor will remain stationary. In other words, it is the flow velocity at which the rotor is on the verge of the beginning of rotation. For this critical condition, N = 0 and from equation (12) and (13) one obtains

$$V_0 = B = \frac{bT_0}{\sqrt{\rho\gamma}\,D^{7/2}} \qquad (14)$$

where V_0 = the threshold velocity. Examination of equation (14) shows that threshold velocity depends on the static resistance torque T_0, the fliud density ρ, the rotor diameter D and a dimensionless experimental coefficient b.

The most important variable is the resistance torque T_0. According to equation (14) one can expect that the threshold velocity will increase as the resistance T_0 increases. Clearly, for best performance, T_0 should be kept as small as possible. In the case of the Price meter, the dependence of the threshold velocity on the static resistance torque has significant implications. The standard Price meter has "cat-whisker" electrical contact brushes which form part of the pulse signal circuit. The overall resistance torque T_0 is strongly dependent on how snugly these contact brushes are set. It is therefore important that the adjustments and settings made at the time of meter calibration are maintained during use in the field.

Equation (14) also shows that the threshold velocity is inversely proportional to the rotor diameter. Therefore for a given resistance T_0, the threshold velocity can be significantly decreased by a small increase in the rotor diameter. For the Price "Pygmy" meter, having an effective rotor diameter of 3.1 cm, the threshold velocity is of the order of 7 cm/s. In contrast to this, for the standard Price meter, having an effective rotor diameter of 7.6 cm, the threshold velocity is of the order of 2 cm/s.

The effect of the fluid density on the threshold velocity can be seen in Figure 5 in which data for calibrations of a Price meter in both air and water are plotted as V vs. N. It is quite clear that the threshold velocity for the meter when the fluid is air is much larger than when the fluid is water. Fortunately, changes in density of the water, as a result of temperature changes are small relative to the density differences between air and water. As a result the density of the water does not affect the response of the meter rotor significantly.

2.2.3 The effect of k

The exponent kN in equation (10) is dimensionless and therefore k has the units of s/rev. Physically, k is a decay constant, the magnitude of which dictates the rate at which the non-linear component of equation (12) approaches the linear component. For a given value of B, the component with the largest value of k will have the largest rate of decline.

The rate of change of the non-linear component reflects the rate of change of the resistance in the meter. Therefore, one can expect that a meter with a high static resistance torque T_0 will have a smaller value of k than a meter for which T_0 is smaller. Since the threshold velocity is directly proportional to T_0, then k should be directly related to V_0 . Therefore an increase in V_0 should be reflected by an increase in k as shown schematically in Figure 6.

2.3 Application of the General Calibration Equation

The general calibration equation given as equation (12), is based on physical principles and reflects the importance of the various factors contributing to the performance characteristics of meters with a vertical axis of rotation. A similar equation was developed by Joag and Singh (1976) based on mathematical curve fitting principles alone. Their equation contains a third term which is not expected to provide any additional variance reduction.

The values of A, V_0 and k must be determined for each current meter calibration by fitting equation (12) to the calibration data using "least squares principles".

2.4 "Least Squares" Fit Coefficients

An optimized fit of equation (12) to the calibration data can be obtained by ensuring that the sum of the squared deviations between the observed values of velocity and their estimated values are as small as possible (Stanton, 1961). Mathematically, this is expressed as

$$S = \sum_{i=1}^{n} (V_i - AN_i - Be^{-k}N_i)^2 \tag{15}$$

sum of the squared deviations, n = the total number of data pairs of V_i and N_i and i = the i'th data pair in the range from 1 and n. For the sake of simplicity the subscipts i are dropped and their presence is taken for granted. The sum S is a minimum for the conditions

$$\frac{\partial S}{\partial A} = \frac{\partial S}{\partial B} = \frac{\partial S}{\partial k} = 0 \tag{16}$$

which result in a set of linear equations from which A and B can be expressed in terms of the third coefficient k. The values of A and B are given by

$$A = \frac{(\Sigma Ve^{-kN}) - B\,(\Sigma e^{-2kN})}{(\Sigma Ne^{-kN})} \tag{17}$$

and

$$B = \frac{(\Sigma NV)(\Sigma Ne^{-kN}) - (\Sigma N^2)(\Sigma Ve^{-kN})}{(\Sigma Ne^{-kN})(\Sigma Ne^{-kN}) - (\Sigma N^2)(\Sigma e^{-2kN})} \tag{18}$$

The solution of equations (17) and (18) require a trial and error procedure. A value k is initally assumed and values of A and B are computed. These inital values of A, B and the assumed value of k are then used to solve for the sum S in equation (15). Additional values of k are chosen and the process is repeated until the value of k which gives the minimum value of S has been found. Substitution of this optimum value of k into equations (17) and (18) ensures optimum values of A and B thereby providing the best fit of equation (12) to the calibration data.

3.0 EXPERIMENTAL EQUIPMENT AND PROCEDURE

3.1 Towing Tank

The towing tank used to conduct the calibration tests is constructed of reinforced concrete, is founded on piles and is 122 metres long and 5 metres wide. The full depth of the tank is 3 metres, of which 1.5 metres are below ground level. Normally, the water depth is maintained at 2.7 metres. Concrete was chosen for its strength, stability and to reduce possible vibrations and convection currents.

At one end of the tank is an overflow weir. Waves arising from towed current meters and their suspensions are washed over the crest, thereby reducing wave reflections. Parallel to the sides of the tank perforated beaches serve to dampen lateral surface wave disturbances.

3.2 Towing Carriage

The towing carriage is 3 metres long, 5 metres wide, weighs 6 tonnes and travels on four precision machined steel wheels on carefully aligned steel rails. The carriage is operated in three overlapping speed ranges:

0.5 cm/s	-	6.0 cm/s
5.0 cm/s	-	60 cm/s
50 cm/s	-	600 cm/s

The maximum speed of 600 cm/s can be maintained for 12 seconds. Tachometer generators connected to the drive shafts emit a voltage signal proportional to the speed of the carriage. A feedback control system uses these signals as input to maintain constant speed during tests.

The average speed data for the towing carriage is obtained by recording the voltage pulses emitted from the measuring wheel. This wheel is attached to the frame of the towing carriage and travels on one of the towing tank rails, emitting a pulse for each millimeter of travel. The pulses and measured time are collected and processed to produce an average towing speed with a micro computer data acquisition system. Analysis of the towing speed variability by Engel (1989), showed that for speeds between 20 cm/s and 300 cm/s, the error in the mean speed was less than 0.15% at the 99% confidence level. Occasionally, these tolerances are exceeded as a result of irregular occurrences such as "spikes" in the data transmission system of the towing carriage. Tests with such anomalies are automatically abandonded.

3.3 Meter Suspension

The calibration tests were conducted using three Price type winter meters, each being fastened to a standard 20 mm diameter solid steel suspension rod. The meters were secured to the rods in accordance with standards used by the WSC for meters with rod suspensions. All meters were suspended 30 cm below the water surface. This depth was chosen to avoid surface effects and to create a minimum of drag on the suspension rods, thereby reducing undesirable vibrations. In all cases great care was taken that the meters were always aligned so that their longitudinal axis was parallel to the direction of travel of the towing carriage.

3.4 Meter Preparation

Prior to testing each meter underwent the following inspection:

a) the penta gear was checked to ensure that it was operating freely;

b) the contact brushes were cleaned and adjusted for proper tension to provide good electrical contact;

c) all moving parts were lubricated;

Following the inspection, the meter was hung in a wind tunnel where it was spun for two hours to ensure that the bearings were properly "run in".

3.5 Meter Rotors

The meter rotors consist of an assembly of six conical cups oriented about a vertical axis of rotation as shown in Figure 1. The rotors are fabricated out of sheet brass with the whole assembly being protected with chrome or nickel plating. The behaviour of this type of rotor has been extensively examined by Engel (1976), Engel and Dezeeuw (1978), Engel and Dezeeuw (1979), Engel and Dezeeuw (1981), Engel and Dezeeuw (1983), Engel and Dezeeuw (1984).

3.6 Test Procedure

A run with the towing carriage at a particular pre-set speed was defined as a test. One set of tests was conducted using three selected metallic rotors with the winter meter yoke. To begin a set of tests each of the three meters was properly aligned in its specified position at the back of the towing carriage. The meters were then towed at pre-selected speeds. Tests were conducted beginning at velocities of 6cm/s up to a maximum of 300 cm/s for a total of 34 tests. Each time the meters were towed, care was taken that steady state conditions prevailed when measurements were recorded. The lengths of the waiting times between successive tests were in accordance with criteria established by Engel and Dezeeuw (1977) or better. For each test, the towing speed, revolutions of the meter rotors and the measuring time were recorded. Water temperatures were not noted because temperature changes during the tests were small and do not affect the performance of the meters (Engel, 1976). The data are recorded in Table 1.

4.0 DATA ANALYSIS

4.1 Non-Linearity in the Meter Response

It was demonstrated in Figure 3 that the non-linearity in the calibration equation can be best revealed by a plot of ND/V vs. V. Considering that, for a given meter, D is constant, an equivalent plot of N/V vs. V can be constructed. The data in Table 1 were used to compute values of N/V for the given values of V and these are plotted as N/V vs. V in Figures 7,8 and 9 for meters No. 1,2, and 3 respectively. The plots clearly show the non-linearity in the meter response, which is greatest at the lowest velocity and decreases as the velocity increases. The rate of change in N/V becomes imperceptively small as velocities become greater than 60 cm/s.

4.2 "Least Squares" Fit of New Calibration Equations

The data in Table 1 were used to obtain a "least squares" calibration equation for each of the three meters used using the procedure described in section 2.4. The values of A, V_0 and k for each of the equations are given in Table 2. The equations were super-imposed on the data plotted as N/V vs. V in Figures 7, 8 and 9. The plots show that the calibration equations duplicate the nonlinear segment of the curves very well, indicating that the form of equation (15) is correct. The small departures in data points from the calibration curve appear to be cyclical, implying the existence of some systematic condition in the towing tank during the calibration of the meters. The source of this effect should be determined by additional tests.

Examination of the results in Table 2 show that there are only very small variations in the values of A and V_0 for the three meters. The values of A represent the geometry and drag characteristics of the rotors. The small variations in A show that all three rotors are virtually identical. The values of V_0 reflect the static resistance T_0 in the meters. The variations in V_0 for the three meters are quite small indicating that the meters have been adjusted approximately the same. Examination of the values of k shows that there is only a small difference between meters #1 and #2 corresponding to a small change in V_0. However, for meter #3, the change in V_0 is larger whereas the corresponding change in k is substantial. Further comparison of k and V_0 shows that k increases as V_0 increases and the sudden change in k for meter #3 relative to meters #1 and #2, shows that k is quite sensitive to changes in V_0. This observation agrees with the schematic trends shown in Figure 6. As values of V_0 increase, k increases resulting in an increase of the curvature of the frictional component of equation (5).

For well adjusted current meters, values of V_0 should not be expected to vary widely from one meter to another. Consequently, the range of k must also be limited. As a result and because the frictional component of equation (12) decays exponentionally, the most significant non-linearity of the calibration curve is confined to velocities less than 60 cm/s. This is confirmed by Figures 7, 8 and 9.

4.3 Comparison of Calibration Equations

The WSC has a large number of current meters. Operationally, it is desirable to develop a current meter calibration with as small a set of data obtained in the towing tank as possible. Presently, the WSC uses 20 data pairs of towing velocity and revolutions per second of the meter rotor to develop its linear calibration equation for each meter. The USGS uses two linear equations with a data set of 10 pairs. One equation is fitted to the data for $N < 1$ and the second equation is used for $N > 1$. In order to conduct a consistent comparison among the new calibration equation and the methods used by the WSC and the USGS, a data set of 20 pairs was selected which is considered to be a realistic representation of the full velocity range used. In all cases calibration equations were fitted to these data using " least squares " principles. The new data set is given in Table 3.

The data in Tables 3 were plotted in Figures 10, 11 and 12 as N/V vs. V together with the values of N/V for the new calibration equations and the equations of the WSC and USGS methods. The curves show that the new calibration equation and the curves obtained with the WSC and USGS methods differ significantly in the low velocity region. The difference is greatest at the lowest velocity and decreases as the velocities increase. At velocities greater than about 30 - 40 cm/s there is no apparent difference in the three curves. The curves also show that the USGS method gives better results than the WSC method. This is due to the fact that with the USGS method greater variance reduction is achieved by the use of the two linear equations than can be obtained with the single linear equation used in the WSC method.

It is clear that the use of linear equations to approximate the true performance characteristics of the current meter results in significant over-estimations of the true velocity at velocities less than 30 - 40 cm/s. The use of equation (15) provides a significant improvement in the low velocity range while maintaing good agreement at velocities greater than 30 - 40 cm/s.

4.4 " Batch " Current Meter Calibration

The fact that k increases as V_0 increases and k is an exponential decay constant, the direct relationship between k and V_0 has a compensating effect. This property is very useful for the development of a "batch" calibration curve. A "batch" relationship between k and V_0 can be developed from a sufficiently large number of current meters. Then, in order to obtain a calibration curve for a particular meter, one need only obtain the mean threshold velocity for that meter based on, say, 10 samples and obtain the corresponding value of k from the "batch" k vs V_0 relationship. Using these average values of k and V_0 and the average "batch" value of A, the calibration curve for a particular meter can be obtained using equation (12). Tests should be conducted using a sample of 50 meters of the same type to investigate the precision that can be achieved with a "batch" calibration curve.

5.0 CONCLUSIONS

In this study a new calibration equation has been developed which effectively takes into account the non-linear frictional segment of the meter rotor response for velocities less than about 40 cm/s. The equation has been developed with the aid of physical arguments and dimensional analysis. The following conclusions have been reached.

5.1 The calibration for the Price current meter can be considered to be composed of a frictionless linear component and a non-linear component which accounts for the frictional properties of the meter. The calibration equation for the Price meter can be expressed as the sum of these two components.

5.2 The most significant non-linearity of the calibration curve is confined to velocities less than about 60 cm/s. For velocities greater than 60 cm/s, the calibration curve is effectively linear. The slope of the linear component represents the equivalent pitch of the meter and is dependent on the shape and orientation of the conical elements of the rotor. The threshold velocity is dependent on the static resistance torque as a result of bearing friction and initial setting of electrical contact brushes on the shaft of the meter rotor. In addition, the threshold velocity is inversely proportional to the effective rotor diameter and the density of the fluid. For normal applications in water, effects of density on the threshold velocity are insignificant.

5.3 The new calibration equation expressed as equation (12) provides an excellent fit to calibration data obtained for rod suspended Price meters. The new equation has the advantage of describing the actual behaviour of the meter rotor throughout the full operating range of the meter as evidenced by the good fit to the calibration data. No subjective judgements associated with fitting of two or more linear equations to selected segments of the calibration data are required.

5.4 "Least squares" fit of equation (12) to the calibration data will provide more accurate computations of velocities at velocities less than about 40 cm/s than can be obtained by the single linear equation used by the WSC and the two linear equations used by the USGS. At velocities greater than 40 cm/s all three methods give about the same results.

5.5 It is anticipated that equation (12) will lend itself more readily for the implementation of a "batch calibration" than presently used linear equations because of its superior performance at velocities less than 40 cm/s.

5.6 Tests should be conducted to determine if a relationship can be established between k and V_0. The possibilty of establishing a current meter calibration based on the threshold velocity and the k vs. V_0 relationship should be investigated .

ACKNOWLEDGEMENT

The calibrations were conducted by C. Bil and B. Near. The data processing was done by D. Doede. The writer is grateful for their enthusiastic support.

REFERENCES

Engel, P. 1976. A Universal Calibration Equation for Price Meters and Similar Instruments. Environment Canada, Inland Waters Directorate, Canada Centre for Inland Waters, Scientific Series No. 65.

Engel, P. and Dezeeuw, C. 1977. Determination of Waiting Times Between Successive Runs when Calibrating Price 622 AA Type Current Meters in a Towing Tank. Technical Note, Hydraulics Research Division, Canada Centre for Inland Waters, Burlington, Ontario.

Engel, P. and Dezeeuw, C. 1978. The Effect of Horizontal Alignment on the Performance of the Price 622 AA Current Meter. Hydraulics Division, National Water Research Institute, Canada Centre for Inland Waters, Burlington, Ontario.

Engel, P. and Dezeeuw, C. 1979. The Effect of Vertical Alignment on the Performance of the Price 622 AA Current Meter. Hydraulics Division, National Water Research Institute, Canada Centre for Inland Waters, Burlington, Ontario.

Engel, P. and Dezeeuw, C. 1981. Sensitivity of the Price Current Meter to Frazil Ice. Hydraulics Division, National Water Research Institute, Canada Centre for Inland Waters, Burlington, Ontario.

Engel, P. and C. Dezeeuw, C. 1983. The Effect of Transverse Velocity Gradients on the Performance of the Price Current Meter. Hydraulics Division, National Water Research Institute, Canada Centre for Inland Waters, NWRI Contribution 83 - 15, Burlington, Ontario.

Engel, P. and Dezeeuw, C. 1984. The Effect of Columbus Type Sounding Weights on the Performance of the Price Current Meter. Hydraulics Division, National Water Research Institute, Canada Centre for Inland Waters, NWRI Contribution 84 - 30, Burlington, Ontario.

Engel, P. 1989. Preliminary Examination of the Variability of the Towing Carriage Speed. Research and Applications Branch, National Water Research Institute, Canada Centre for Inland Waters, NWRI Contribution 89 - 89., Burlington, Ontario.

Rouse, H., Editior, (1950). Engineering Hydraulics. Proceedings of the Fourth Hydraulics Conference, Iowa Institute of Hydraulic Research, June 12 - 15, 1949. John Wiley & Sons, Inc. New York.

Joag, A.P. and Singh, D.P. 1976. Evolution of a Uniform Current Meter Rating Curve. Diamond Jubilee Symposium, Central Water Power Research Station, India.

Schubauer, G.B. and Mason, M.A. 1937. Performance Characteristics of a Current Meter in Air. Journal of the National Bureau of Standards, Volume 18.

Smoot, G.F. and Carter, R.W. 1968. Are Individual Current Meter Ratings Necessary ?, Journal of the Hydraulics Division, ASCE, Vol. 94, No. HY2.

Stanton, R.G. 1961. Numerical Methods for Science and Enginering. International Series in Engineering, Prentice - Hall of Canada Limited.

TABLE 1

CALIBRATION DATA SET

V cm/s	Meter # AAW1 N rev/s	Meter # AAW2 N rev/s	Meter # AAW4 N rev/s
3.01	0.031	0.031	0.032
6.01	0.075	0.075	0.075
9.09	0.122	0.120	0.120
12.05	0.164	0.164	0.164
15.09	0.208	0.209	0.209
18.07	0.252	0.253	0.253
21.00	0.298	0.299	0.298
24.06	0.344	0.346	0.340
27.06	0.390	0.390	0.388
30.04	0.430	0.433	0.429
36.07	0.524	0.526	0.524
42.02	0.611	0.611	0.609
48.02	0.697	0.701	0.696
54.08	0.778	0.787	0.781
60.17	0.866	0.872	0.866
66.57	0.959	0.968	0.958
72.52	1.053	1.058	1.050
78.64	1.141	1.144	1.142
84.77	1.239	1.242	1.236
90.64	1.316	1.322	1.316
105.34	1.532	1.537	1.531
120.37	1.747	1.753	1.752
135.44	1.975	1.979	1.981
149.92	2.188	2.193	2.187
165.79	2.424	2.429	2.425
180.28	2.632	2.637	2.634
195.63	2.854	2.867	2.856
210.15	3.067	3.074	3.076
225.61	3.295	3.303	3.298
240.51	3.519	3.535	3.519
255.49	3.729	3.750	3.737
270.31	3.943	3.957	3.956
285.56	4.158	4.182	4.165
300.79	4.373	4.384	4.367

TABLE 2

VALUES OF A,V AND k FOR LONG DATA SET

Constant	Meter # AAW1	Meter # AAW2	Meter # AAW4
A	68.566	68.315	68.454
V	0.918	0.929	0.835
k	1.211	1.285	0.594

The units of A are cm/rev
The units of B are cm/s
The units of k are s/rev

TABLE 3

REDUCED CALIBRATION DATA SET

	Meter # AAW1	Meter # AAW2	Meter # AAW4
V cm/s	N rev/s	N rev/s	N rev/s
6.01	0.075	0.075	0.075
12.05	0.164	0.164	0.164
18.07	0.252	0.253	0.253
24.06	0.344	0.346	0.340
30.04	0.430	0.433	0.429
36.07	0.524	0.526	0.524
42.02	0.611	0.611	0.609
48.02	0.697	0.701	0.696
54.08	0.778	0.787	0.781
60.17	0.866	0.872	0.866
84.77	1.239	1.242	1.236
108.28	1.575	1.579	1.578
132.38	1.928	1.933	1.933
156.33	2.273	2.284	2.282
180.28	2.632	2.637	2.634
204.37	2.978	2.988	2.985
228.59	3.340	3.344	3.344
252.21	3.682	3.698	3.687
276.04	4.024	4.039	4.036
300.79	4.373	4.384	4.367

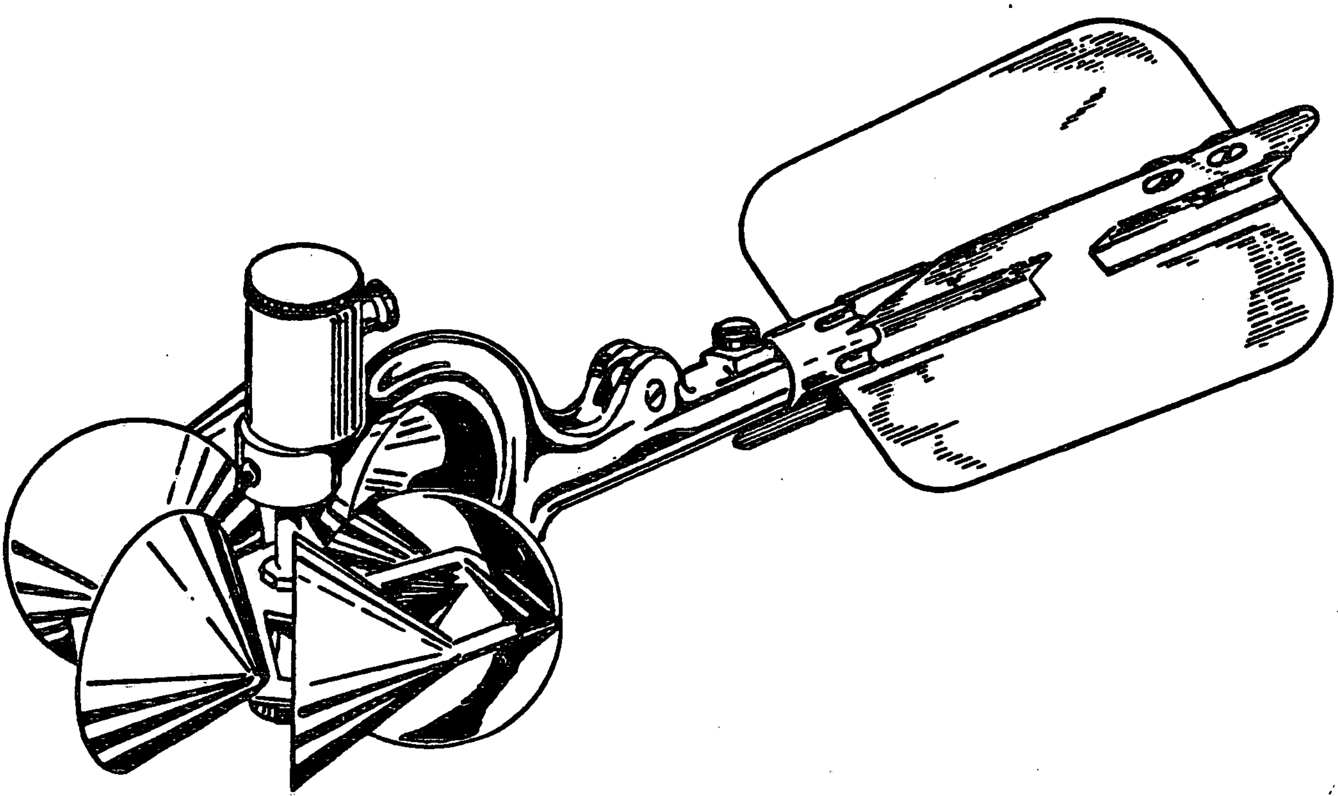

Figure 1. Price Meter with Conventional Rotor.

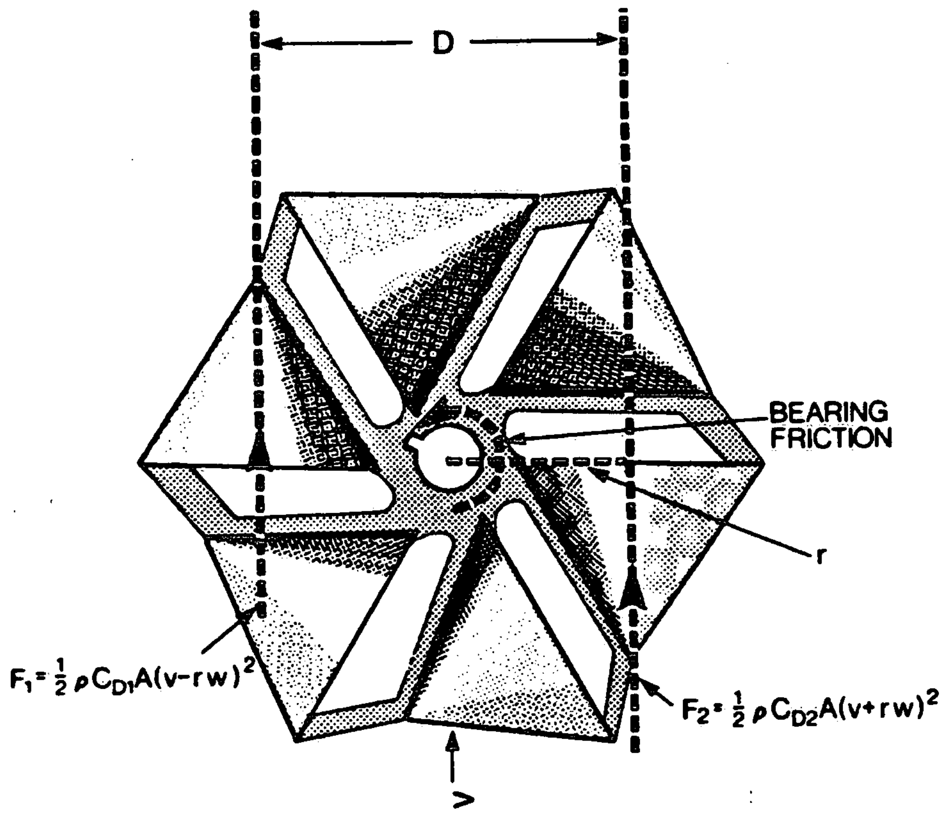

Figure 2. Forces on the Rotor.

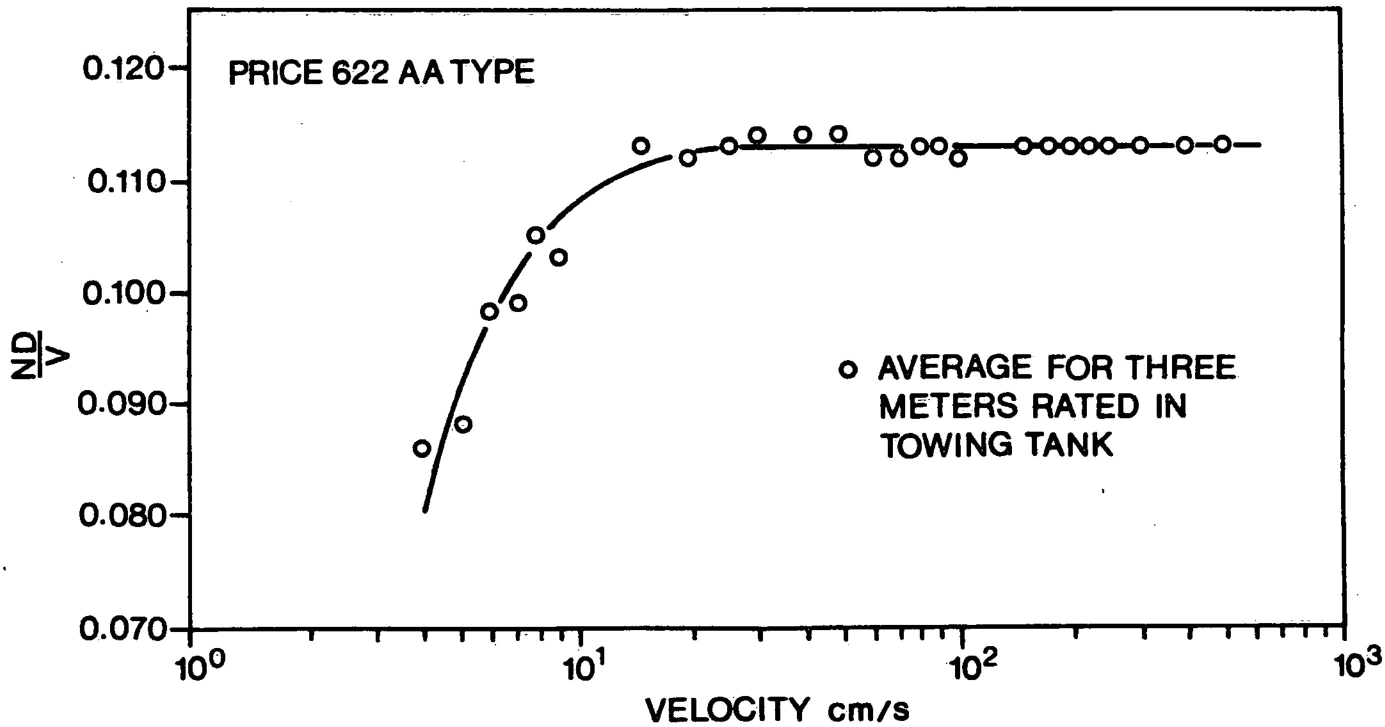

Figure 3. Typical Price Meter Performance Curve.

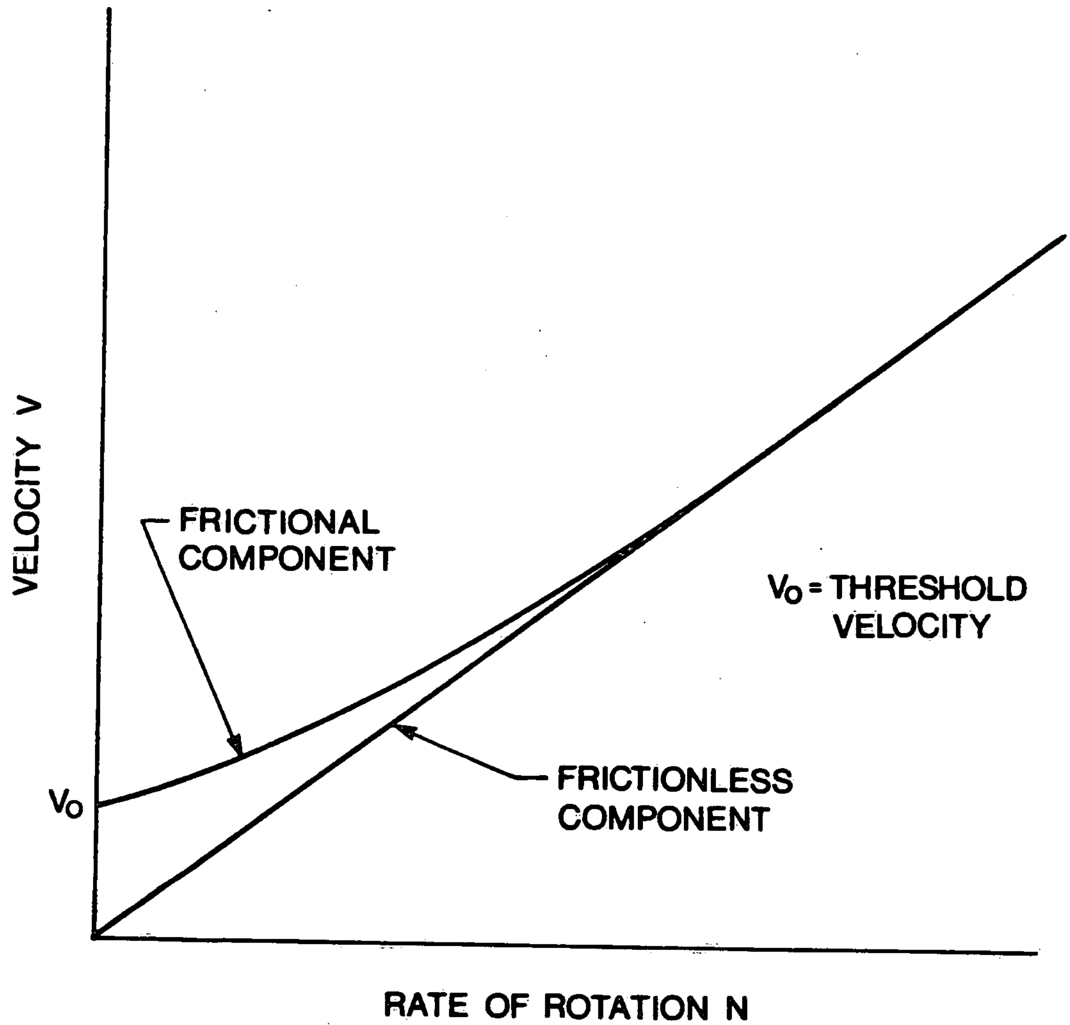

Figure 4. Components of Calibration Equation

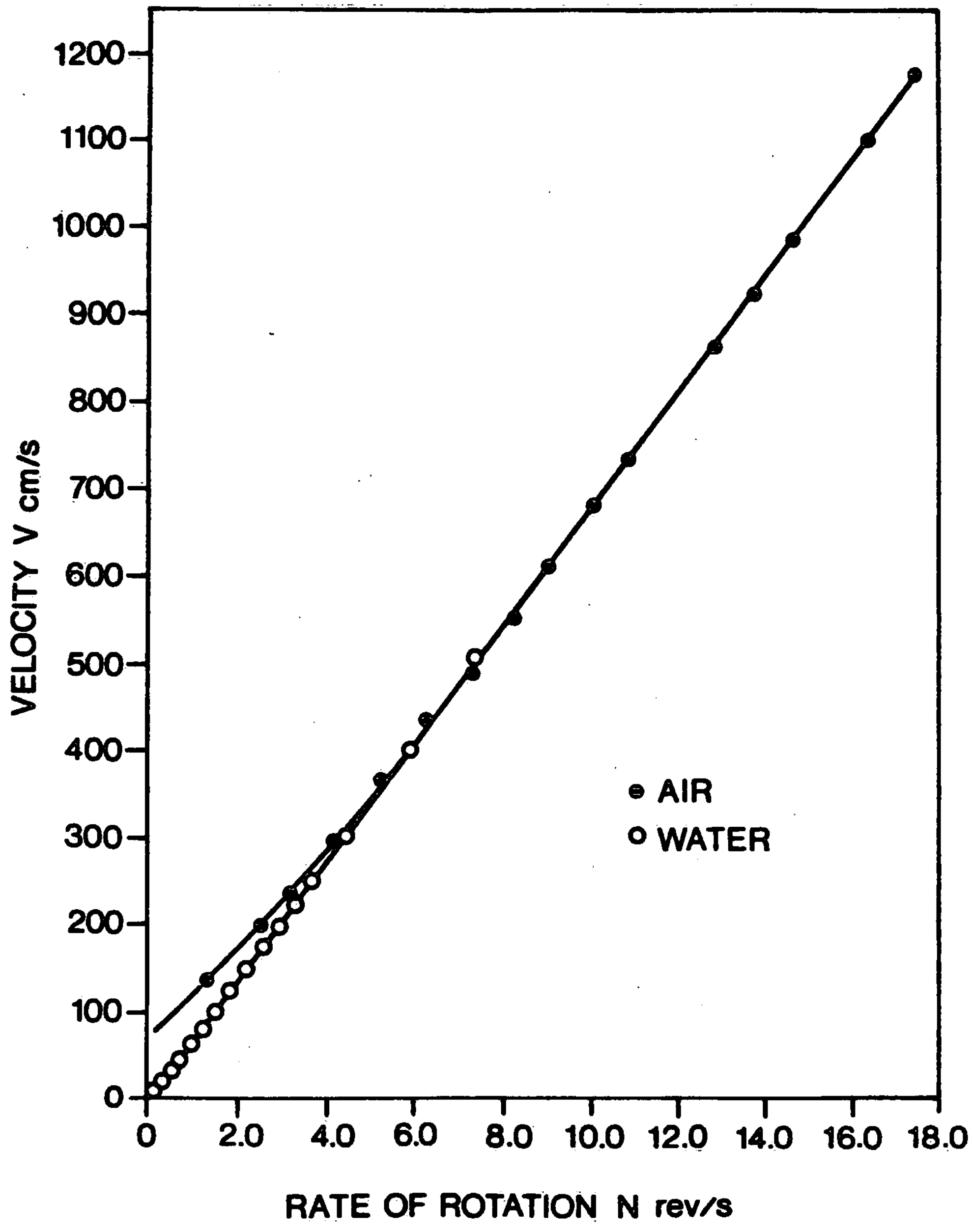

Figure 5. Calibration Curves for Price Meter in Air and Water.

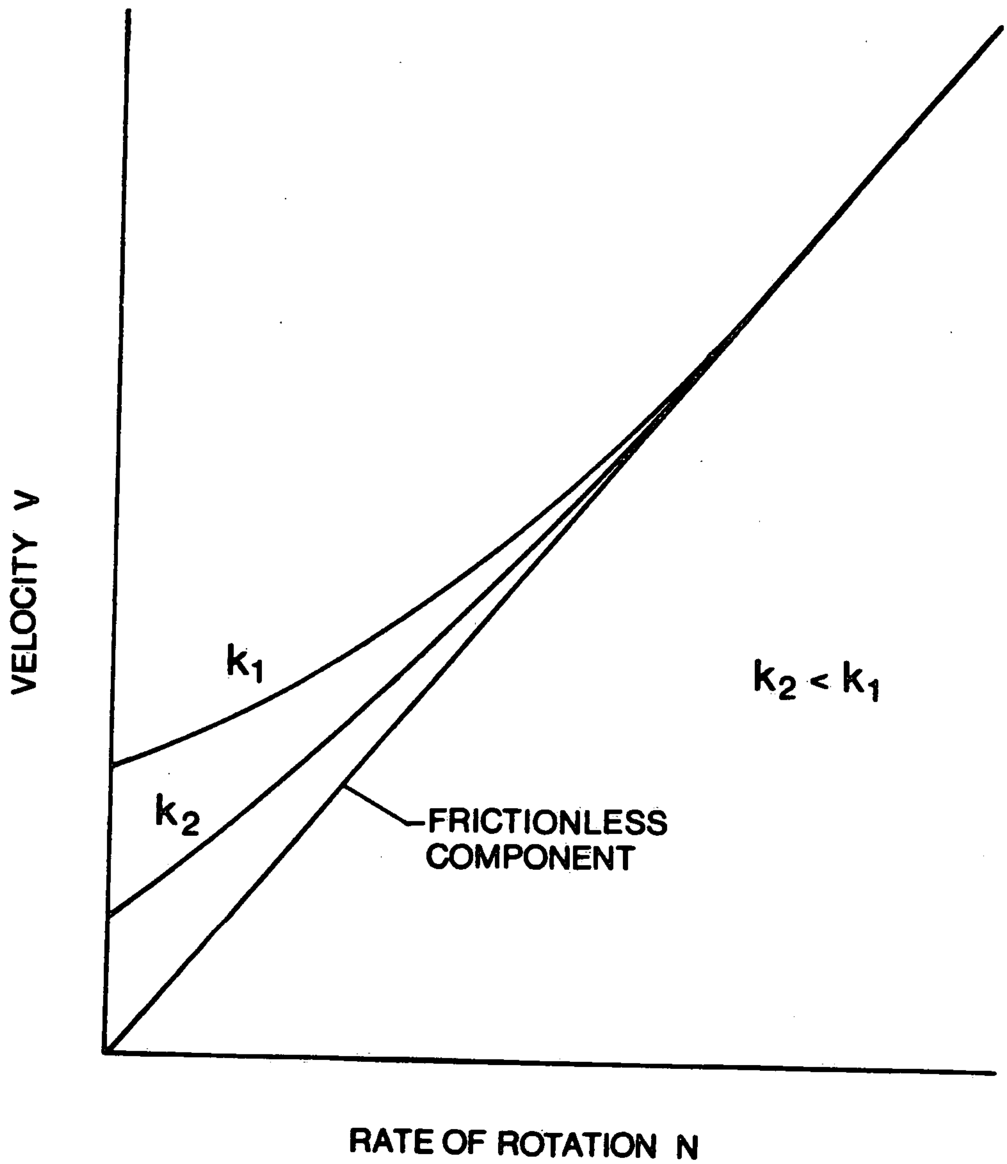

Figure 6. Effect of Decay Constant k.

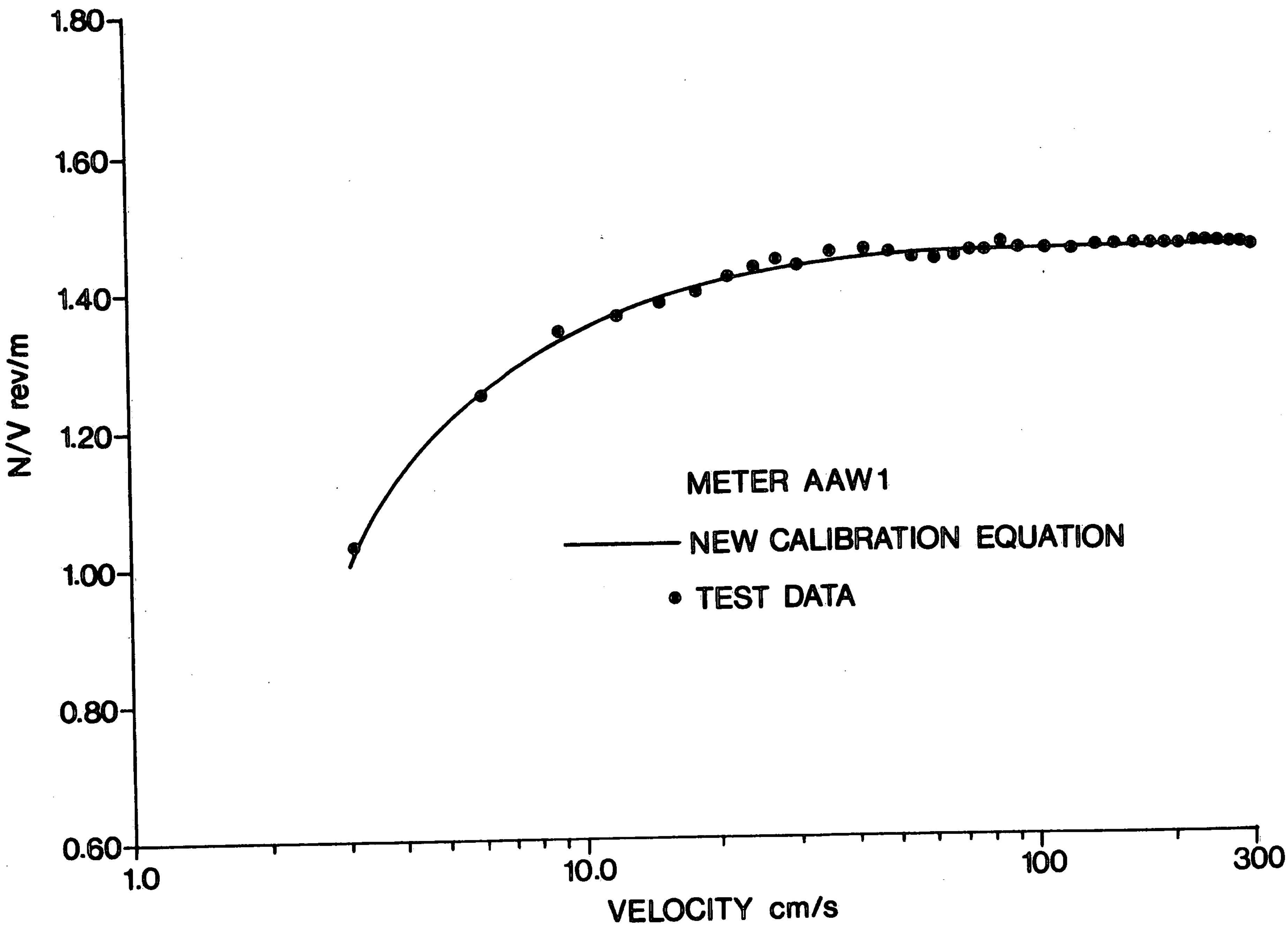

Figure 7. Performance Curve for Meter No. AAW1.

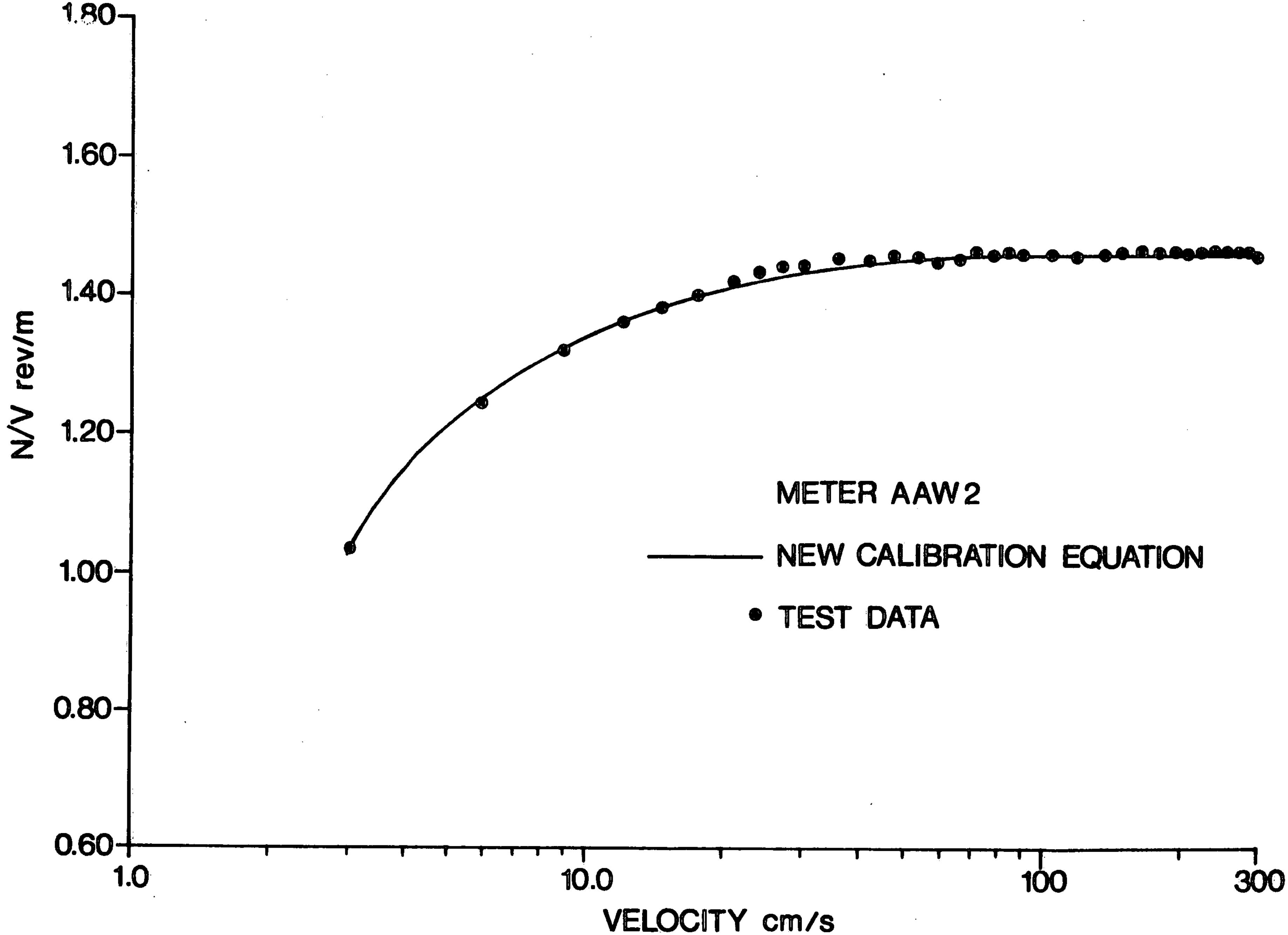

Figure 8. Performance Curve for Meter No. AAW2

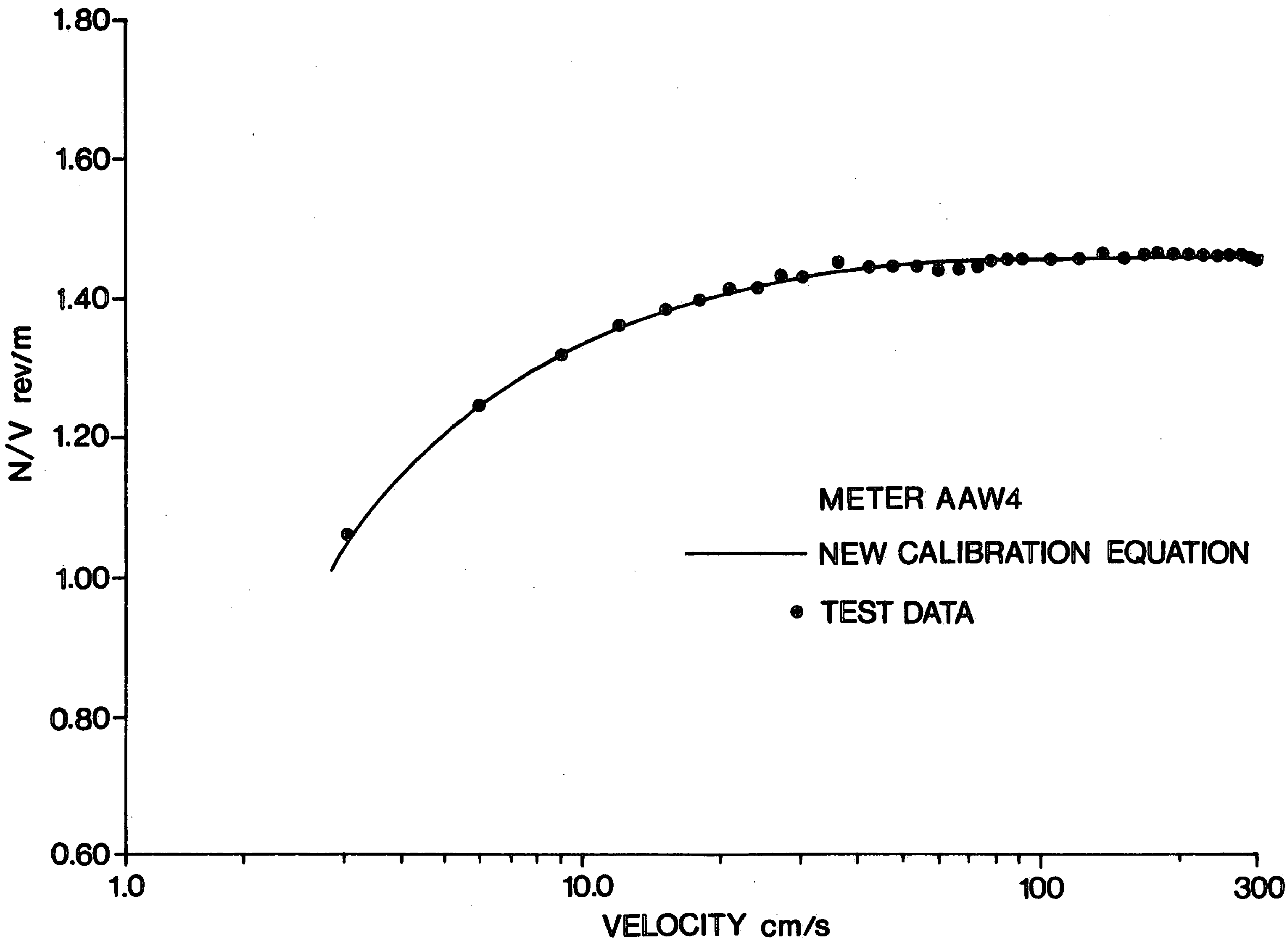

Figure 9. Performance Curve for Meter No. AAW4

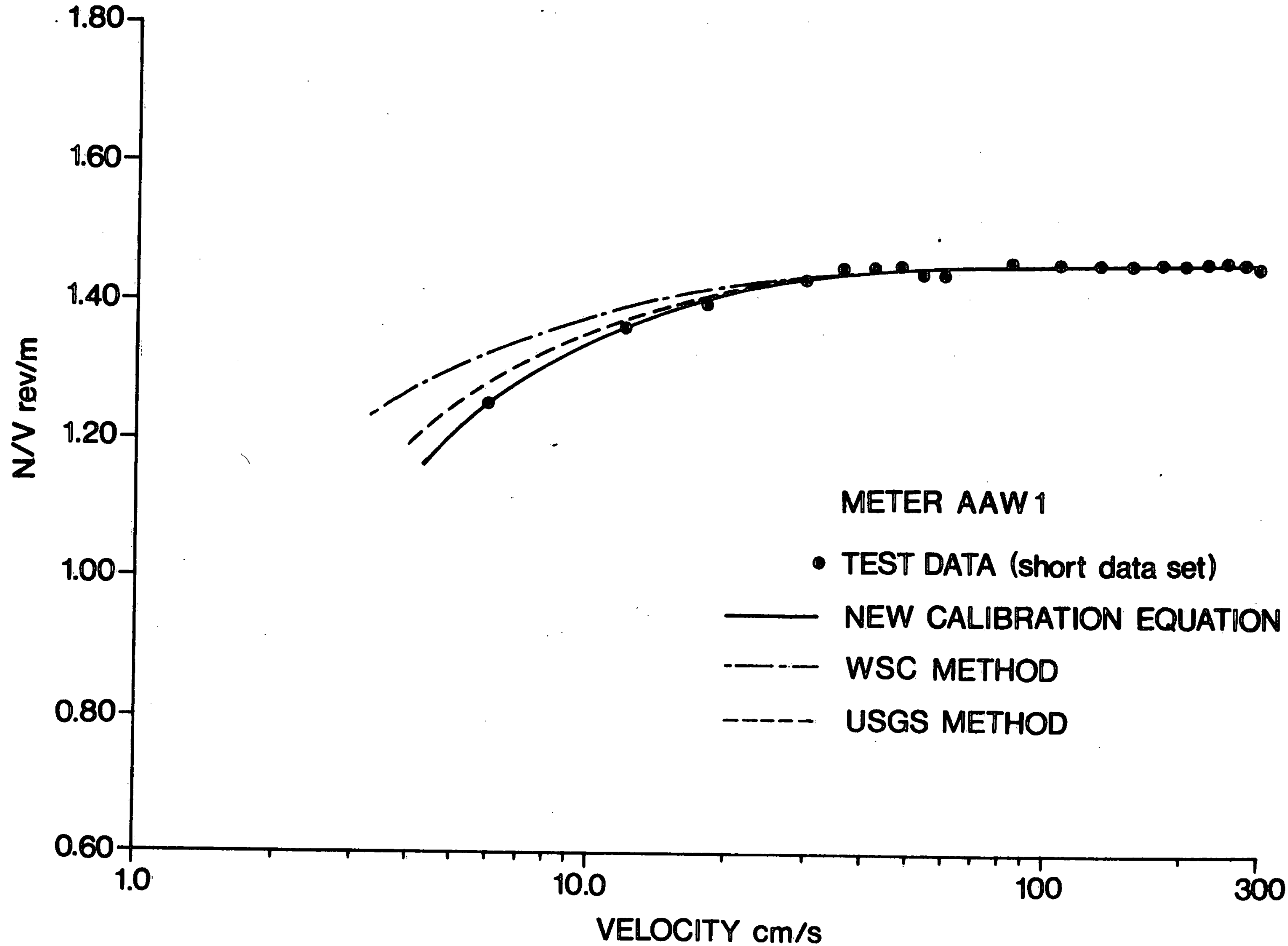

Figure 10. Comparison of Calibration Equations for Meter No. AAW1.

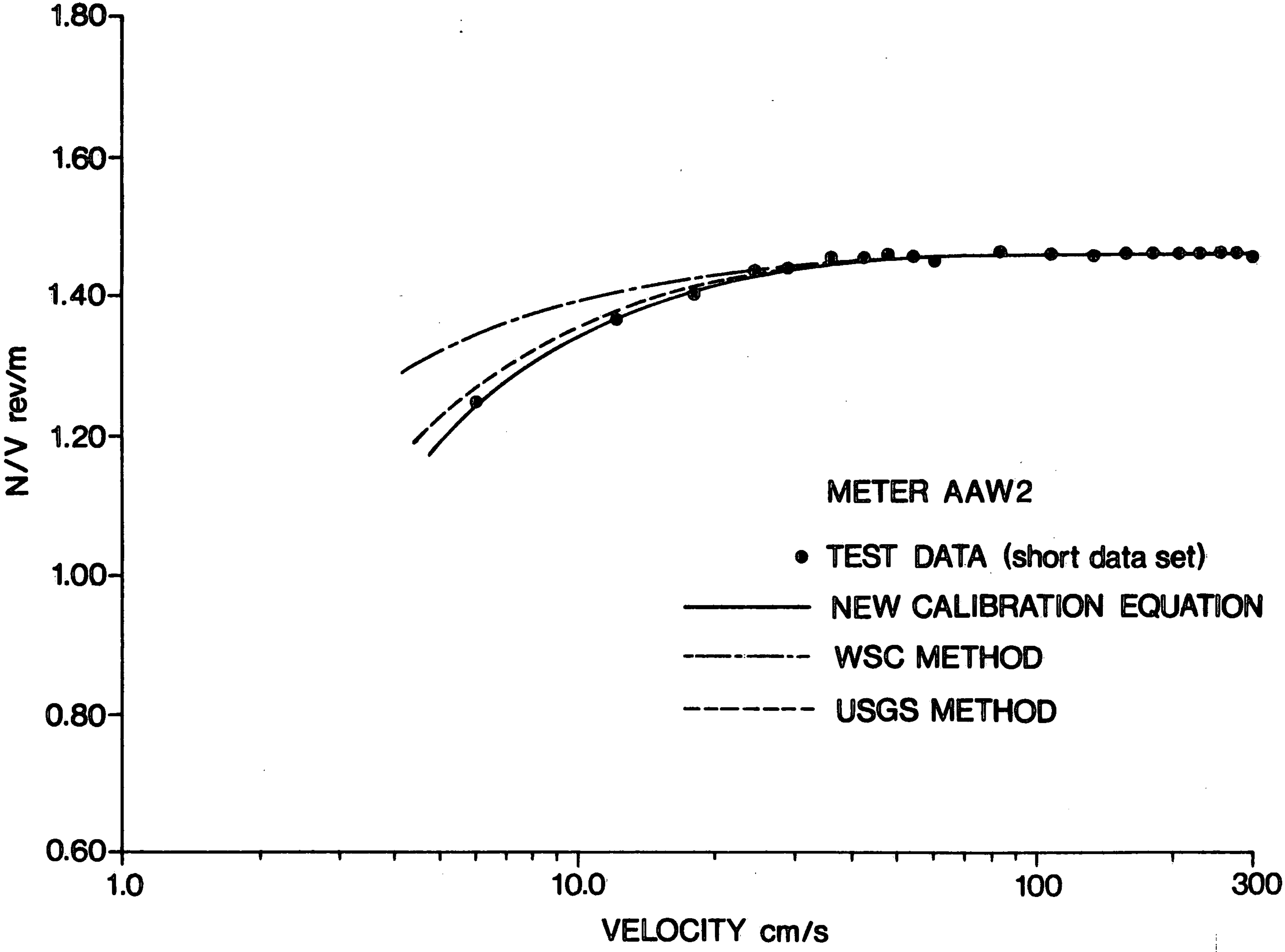

Figure 11. Comparison of Calibration Equations for Meter No. AAW2.

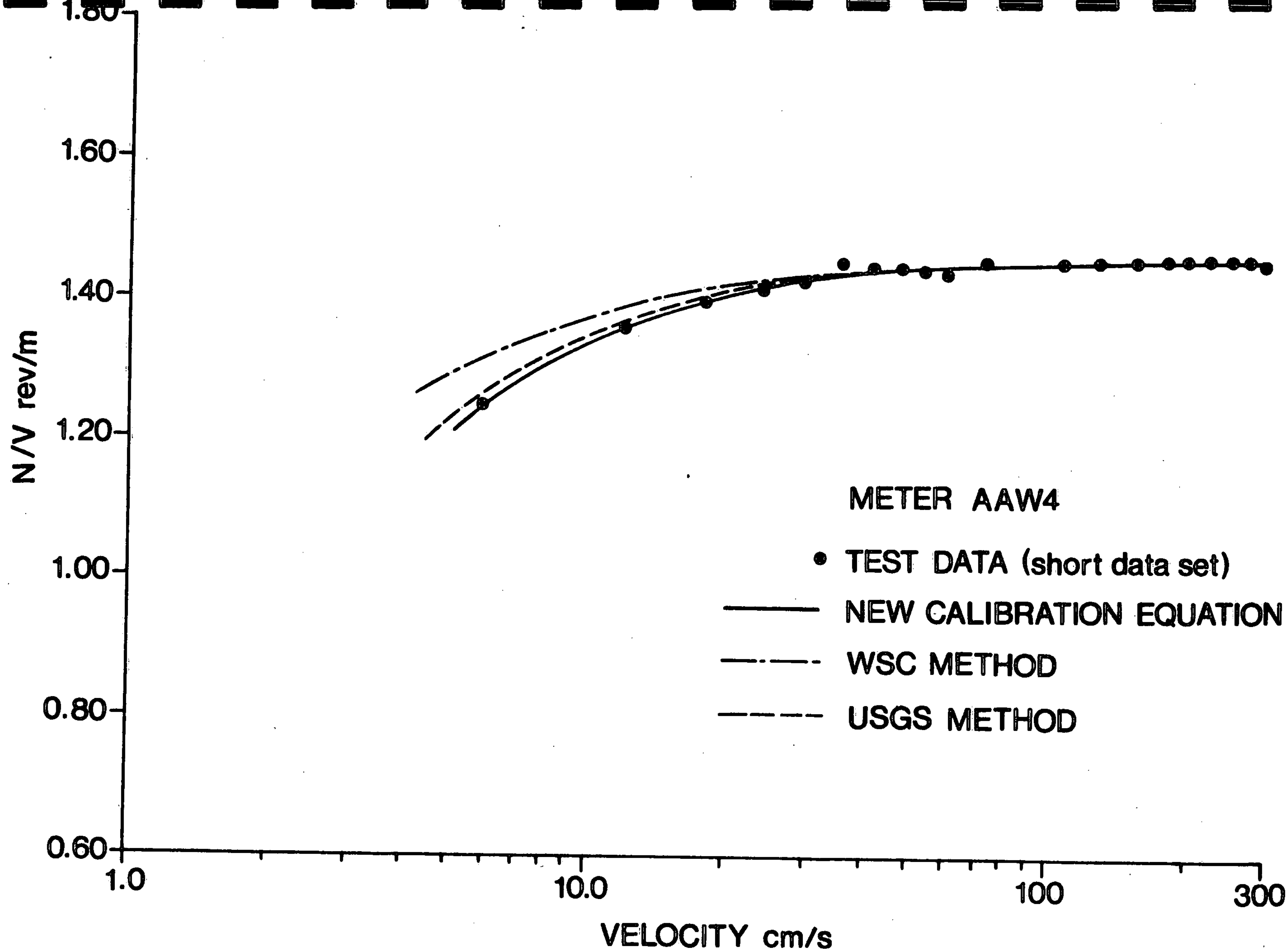

Figure 12. Comparison of Calibration Equations for Meter No. AAW4